

# Insertion of Ethyne into the Ru–B Bond of a Coordinatively Unsaturated Ruthenium Boryl Complex. X-ray Crystal Structure of



George R. Clark, Geoffrey J. Irvine, Warren R. Roper,\* and L. James Wright\*

Department of Chemistry, The University of Auckland, Private Bag 92019, Auckland, New Zealand

Received July 21, 1997<sup>®</sup>

Ethyne inserts readily into the Ru–B bond of the five-coordinate boryl complex  $\text{Ru}(\text{BO}_2\text{C}_6\text{H}_4)\text{Cl}(\text{CO})(\text{PPh}_3)_2$  (**1**) to form the borylalkenyl complex  $\text{Ru}(\text{CH}=\text{CH}[\text{BOC}_6\text{H}_4\text{O}])\text{Cl}(\text{CO})(\text{PPh}_3)_2$  (**2**). Complex **2** has been characterized by IR and multinuclear NMR spectroscopy and by an X-ray crystal structure determination. In the solid state, the Ru atom in **2** is six coordinate through weak attachment of a catechol oxygen to ruthenium. Two further products,  $\text{Ru}(\text{CH}=\text{CHB}[\text{OCH}_2\text{CH}_2\text{O}])\text{Cl}(\text{CO})(\text{PPh}_3)_2$  (**3**) and  $\text{Ru}(\text{CH}=\text{CHB}[\text{OEt}][\text{OEt}])\text{Cl}(\text{CO})(\text{PPh}_3)_2$  (**4**), which result from transesterification of **2** with  $\text{HOCH}_2\text{CH}_2\text{OH}$  and **3** with  $\text{CH}_3\text{CH}_2\text{OH}$ , respectively, are also described. The relevance of the observed ethyne insertion for metal-catalyzed hydroboration is discussed.

## Introduction

Migratory insertion reactions play an essential role in the mechanisms of many late transition metal-catalyzed processes, and for metal-catalyzed hydroboration, the possibility of alkene or alkyne insertion into a M–B bond as a key step must be considered.

In 1985, Männig and Nöth<sup>1</sup> reported that, in the presence of  $\text{RhCl}(\text{PPh}_3)_3$ , catecholborane hydroborated a number of alkenes under very mild conditions with a high degree of chemoselectivity. A variety of transition metal complexes are now known to effectively catalyze the hydroboration of alkenes and alkynes, and many examples are derivatives of the platinum group metals.<sup>2</sup> The most commonly employed catalysts are those of rhodium. In addition to offering rate enhancements, the catalyzed reactions afford substantially modified chemo-, regio-, and stereoselectivities when compared to the uncatalyzed reaction.<sup>3a–n</sup>

A widely accepted mechanistic pathway for the hydroboration of alkenes catalyzed by platinum group metals is that first proposed by Männig and Nöth. This

mechanism is very similar to the more thoroughly studied rhodium-catalyzed hydrometalation reactions, namely, hydroformylation, hydrogenation, and hydrosilylation.<sup>4</sup> The mechanism involves initial oxidative addition of the B–H bond to  $\text{Rh}(\text{I})$ , followed by alkene coordination and subsequent insertion into the Rh–H bond to afford a mixed alkyl, boryl complex. Reductive deborylation via B–C elimination then liberates the hydroborated product and regenerates the catalyst. Support for this mechanism has been afforded by stoichiometric reaction chemistry.  $\text{RhHCl}(\text{BO}_2\text{C}_6\text{H}_4)(\text{PPh}_3)_2$ ,<sup>5</sup> which is readily generated by treatment of  $\text{RhCl}(\text{PPh}_3)_3$  with catecholborane, reacts stoichiometrically with alkenes, resulting in hydroboration and regeneration of  $\text{RhCl}(\text{PPh}_3)_3$ .<sup>1</sup> Computational studies have also supported this mechanism.<sup>6h</sup> However, the formation of vinylboranes and vinylboronate esters during some metal-promoted B–H additions to alkenes has pointed to the possibility of an alternative mechanistic pathway in which insertion of the alkene into the metal–boron bond occurs in preference to insertion into the metal–hydride bond.<sup>6a–g</sup> In a competing side reaction,  $\beta$ -H elimination from the resulting intermediate borylalkyl complex then affords the vinylborane byproduct. Support for this proposed mechanism was recently obtained

<sup>®</sup> Abstract published in *Advance ACS Abstracts*, November 15, 1997.

(1) Männig, D.; Nöth, H. *Angew. Chem., Int. Ed. Engl.* **1985**, *24*, 878.

(2) Burgess, K.; Ohlmeyer, M. J. *Chem. Rev.* **1991**, *91*, 1179.

(3) (a) Evans, D. A.; Fu, G. C.; Hoveyda, A. H. *J. Am. Chem. Soc.* **1988**, *110*, 6917. (b) Hayashi, T.; Ito, Y.; Matsumoto, Y. *J. Am. Chem. Soc.* **1989**, *111*, 3426. (c) Brown, J. M.; Lloyd-Jones, G. C. *Tetrahedron: Asymmetry* **1990**, *1*, 869. (d) Miyaoura, N.; Sato, M.; Suzuki, A. *Tetrahedron Lett.* **1990**, *31*, 231. (e) Evans, D. A.; Fu, G. C. *J. Am. Chem. Soc.* **1991**, *113*, 4042. (f) Hayashi, T.; Matsumoto, Y. *Tetrahedron Lett.* **1991**, *32*, 3387. (g) Harrison, K. N.; Marks, T. J. *J. Am. Chem. Soc.* **1992**, *114*, 9220. (h) Baker, R. T.; Calabrese, J. C.; Marder, T. B.; Taylor, N. J.; Westcott, S. A. *J. Am. Chem. Soc.* **1992**, *114*, 8863. (i) Evans, D. A.; Fu, G. C.; Hoveyda, A. H. *J. Am. Chem. Soc.* **1992**, *114*, 6671. (j) Hayashi, T.; Matsumoto, Y.; Naito, M. *Organometallics* **1992**, *11*, 2732. (k) Gridnev, I. D.; Miyaoura, N.; Suzuki, A. *Organometallics* **1993**, *12*, 589. (l) Pereira, S.; Srebnik, M. *Organometallics* **1995**, *14*, 3127. (m) Baker, R. T.; Calabrese, J. C.; Westcott, S. A. *J. Organomet. Chem.* **1995**, *498*, 109. (n) Iverson, C. M.; Smith, M. R., III. *J. Am. Chem. Soc.* **1995**, *117*, 4403.

(4) Collman, J. P.; Finke, R. G.; Hegedus, L. S.; Norton, J. R. *Principles and Applications of Organotransition Metal Chemistry*; University Science: Mill Valley, CA, 1987.

(5) Ito, K.; Kono, H.; Nagai, Y. *Chem. Lett.* **1975**, 1095.

(6) (a) Corcoran, E. W., Jr.; Davan, T.; Sneddon, L. G. *Organometallics* **1983**, *2*, 1693. (b) Lynch, A. T.; Sneddon, L. G. *J. Am. Chem. Soc.* **1989**, *111*, 6201. (c) Brown, J. M.; Lloyd-Jones, G. C. *J. Chem. Soc., Chem. Commun.* **1992**, 710. (d) Baker, R. T.; Calabrese, J. C.; Marder, T. B.; Nguyen, P.; Westcott, S. A. *J. Am. Chem. Soc.* **1993**, *115*, 4367. (e) Baker, R. T.; Marder, T. B.; Westcott, S. A. *Organometallics* **1993**, *12*, 975. (f) Baker, R. T.; Blom, H. P.; Calabrese, J. C.; Marder, T. B.; Nguyen, P.; Taylor, N. J.; Westcott, S. A. In *Current Topics in the Chemistry of Boron*; Kabalka, G. W., Ed.; Royal Society of Chemistry: Cambridge, U.K., 1994; pp 68–71. (g) Mebel, A. M.; Morokuma, K.; Musaev, D. G. *J. Am. Chem. Soc.* **1994**, *116*, 10693. (h) Dorigo, A. E.; Schleyer, P. v. R. *Angew. Chem., Int. Ed. Engl.* **1995**, *34*, 115.

from a study which compared alkene insertion into the iridium–hydrogen or iridium–boron bonds of suitable model compounds.<sup>7</sup> It was found that insertion into the Ir–B bond was thermodynamically slightly more favorable than insertion into the Ir–H bond. However, in this particular case, the close similarity in  $\Delta H$  terms for each insertion process suggested that there could be competition between the two insertion pathways and that kinetic factors would determine selectivity between them. Additional support for the feasibility of alkene insertion into metal–boron bonds during metal-catalyzed hydroboration comes from two recent studies of alkene or alkyne insertion into M–B bonds in which the presence of borylalkyl or borylalkenyl intermediates were clearly indicated.<sup>6d,8</sup>

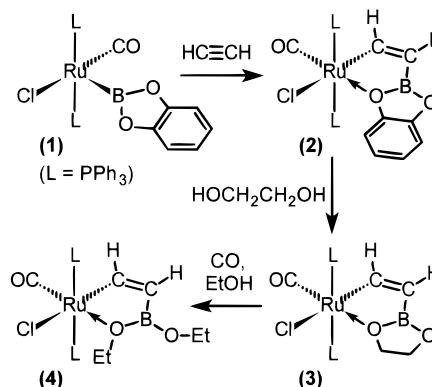
Recently it was suggested that it may be necessary to consider yet another mechanistic variation in some cases. Hartwig and co-workers found that treatment of  $\text{CpRu}(\text{Me})(\text{PPh}_3)_2$  with catecholborane in arene solvent at room temperature produced  $\text{CpRu}(\text{H})(\text{PPh}_3)_2$  and methylcatecholborane quantitatively. On careful study of this reaction, strong evidence was obtained that the B–C bond formation step did not proceed via a sequence of oxidative and reductive steps but rather via a  $\sigma$ -bond metathesis pathway.<sup>9</sup>

Few mechanistic investigations have appeared that address catalytic alkyne hydroboration, but more attention has been directed toward metal-catalyzed diborylation of alkynes.<sup>10a–d</sup> It seems likely that alkyne insertion into a metal–boron bond is a key step in both of these processes. Although considerable evidence for the intermediacy of borylalkyl and borylalkenyl moieties in alkene and alkyne insertion, respectively, has been obtained, as yet no stable examples of such species resulting from the corresponding stoichiometric reactions have been isolated.<sup>6d,8</sup> The work reported here describes the synthesis and characterization of the first example of a stable metalated vinyl boronate ester derived from the formal insertion of ethyne into the Ru–B bond of  $\text{Ru}(\text{BO}_2\text{C}_6\text{H}_4)\text{Cl}(\text{CO})(\text{PPh}_3)_2$ .<sup>11</sup> The reactivity of this compound, and the implications for transition metal-catalyzed hydroboration, are also discussed.

## Results and Discussion

**Insertion of Ethyne into the Ru–B Bond of  $\text{Ru}(\text{BO}_2\text{C}_6\text{H}_4)\text{Cl}(\text{CO})(\text{PPh}_3)_2$  (1).** When a benzene solution of **1** was treated with ethyne under low pressure (1 atm), at a temperature of  $\sim 65^\circ\text{C}$ , the initially pale yellow solution turned golden yellow over the course of 20 min. The nearly colorless product, which was isolated in good yield from solution, was formulated as  $\text{Ru}(\text{CH}=\text{CH}[\text{BOC}_6\text{H}_4\text{O}])\text{Cl}(\text{CO})(\text{PPh}_3)_2$  (**2**), where ethyne

**Scheme 1**



has formally inserted into the Ru–B bond (see Scheme 1). Since coordinatively unsaturated  $d^6$  complexes are usually strongly colored, the very pale color of this product suggested that in the solid state the ruthenium center was coordinatively saturated. One way this could be achieved would be by having an oxygen atom of the catecholboryl group interact with the metal center.

The infrared spectrum of **2** displayed a very sharp  $\nu(\text{CO})$  band at  $1915\text{ cm}^{-1}$  which was  $\sim 25\text{ cm}^{-1}$  lower than  $\nu(\text{CO})$  in the starting material **1** but in a position similar to that reported for the alkenyl complex of ruthenium,  $\text{RuCl}(\text{PhC}=\text{CHPh})(\text{CO})(\text{PPh}_3)_2$ .<sup>12</sup> Other significant bands were observed at 1339, 1283, 1246, and  $1227\text{ cm}^{-1}$ . Complete IR data for this and other reported compounds are given in Table 1. A band that could be assigned to  $\nu(\text{C}=\text{C})$  was not readily discernible. However, the presence of the alkenyl moiety was confirmed by NMR spectroscopy (see Tables 2 and 3). Resonances for each of the alkenyl carbon atoms were clearly visible in the  $^{13}\text{C}$  NMR spectrum. The triplet centered at 207.3 ppm ( $J_{\text{CP}} = 10.7\text{ Hz}$ ) was assigned to the metalated alkenyl carbon ( $\text{C}_\alpha$ ), and a broad singlet at 122.2 ppm was assigned to the remote carbon atom ( $\text{C}_\beta$ ). The broadness of this latter signal is consistent with there being a direct connectivity to the quadrupolar boron nucleus. The alkenyl proton resonances were observed in the  $^1\text{H}$  NMR spectrum as two sets of doublets of triplets, one set centered at 5.79 ppm and the other at 9.69 ppm. In each case, this pattern arises from coupling to the two mutually *trans* phosphorus nuclei as well as coupling to the other alkenyl proton. The magnitude of the vicinal H, H coupling constant for the alkenyl protons ( $^3J_{\text{HH}} = 11.7\text{ Hz}$ ) is very close to the normally encountered limits for both (*Z*)- and (*E*)-alkenyl complexes,<sup>13</sup> and so unambiguous assignment of structure on this basis is not possible. However, the results of an X-ray structure determination (see below) clearly show a *Z* geometry about the double bond in the solid state. Assignment of the resonances due to the two alkenyl protons was achieved by examination of the  $^{13}\text{C}$ – $^1\text{H}$  cross-peaks in the 2D ( $^1\text{H}$ , $^{13}\text{C}$ )-COSY spectrum. This showed that the proton that appeared at 9.69 ppm is bonded to the metalated carbon ( $\text{C}_\alpha$ ) whereas the proton that appears at 5.79 ppm is attached to ( $\text{C}_\beta$ ). Both proton resonances show coupling to the two mutually *trans* phosphorus nuclei with  $^3J_{\text{HP}} = 1.3\text{ Hz}$  and  $^4J_{\text{HP}}$

(7) Rablen, P. R.; Hartwig, J. F. *J. Am. Chem. Soc.* **1994**, *116*, 4121.

(8) Ishiyama, T.; Matsuda, N.; Miyaura, N.; Suzuki, A. *J. Am. Chem. Soc.* **1993**, *115*, 11018.

(9) Bhandari, S.; Hartwig, J. F.; Rablen, P. R. *J. Am. Chem. Soc.* **1994**, *116*, 1839.

(10) (a) Ishiyama, T.; Matsuda, N.; Murata, M.; Ozawa, F.; Suzuki, A.; Miyaura, N. *Organometallics* **1996**, *15*, 713. (b) Sakaki, S.; Kikuno, T. *Inorg. Chem.* **1997**, *36*, 226. (c) Lesley, G.; Nguyen, P.; Taylor, N. J.; Marder, T. B.; Scott, A. J.; Clegg, W.; Norman, N. C. *Organometallics* **1996**, *15*, 5137. (d) Iverson, C. N.; Smith, M. R., III *Organometallics* **1996**, *15*, 5155.

(11) Irvine, G. J.; Roper, W. R.; Wright, L. J. *Organometallics* **1997**, *16*, 2291.

(12) Ros, J.; Santos, A.; Torres, M. R.; Vegas, A. *J. Organomet. Chem.* **1986**, *309*, 169.

(13) Maddock, S. M.; Rickard, C. E. F.; Roper, W. R.; Wright, L. J. *Organometallics* **1996**, *15*, 1793.

**Table 1. Infrared Data (cm<sup>-1</sup>)<sup>a</sup> for Ruthenium Complexes**

complex	$\nu(\text{C}\equiv\text{O})$	other bands <sup>b</sup>
$\text{Ru}(\text{CH}=\text{CH}[\text{BOC}_6\text{H}_4\text{O}])\text{Cl}(\text{CO})(\text{PPh}_3)_2$ ( <b>2</b> )	1915 vs	1412 w, 1339 m, 1283 m, 1246 m, 1227, 1192 w, 869 w, 814 w
$\text{Ru}(\text{CH}=\text{CH}[\text{BOCH}_2\text{CH}_2\text{O}])\text{Cl}(\text{CO})(\text{PPh}_3)_2$ ( <b>3</b> )	1907 vs	1492, 1403 m, 1363 m sh, 1247, 1190 m, 1014 m, 945 w, 848 w
$\text{Ru}(\text{CH}=\text{CHB}[\text{OEt}][\text{OEt}])\text{Cl}(\text{CO})(\text{PPh}_3)_2$ ( <b>4</b> )	1914 vs	1490 sh, 1408 w, 1320 m, 1297 m sh, 1266, 1207 m, 1160 w, 1028 m, 885 m, 724 m

<sup>a</sup> All intensities strong unless denoted otherwise. <sup>b</sup> Bands associated with vinyl-boronate ligand.

**Table 2. <sup>1</sup>H NMR Data for Ruthenium Complexes**

complex	<sup>1</sup> H, $\delta$ (ppm) <sup>a</sup>
$\text{Ru}(\text{CH}=\text{CH}[\text{BOC}_6\text{H}_4\text{O}])\text{Cl}(\text{CO})(\text{PPh}_3)_2$ ( <b>2</b> ) recorded at 298 K <sup>b</sup>	5.79 dt, <sup>3</sup> J <sub>HH</sub> = 11.7, <sup>4</sup> J <sub>HP</sub> = 1.8, 1H, CH=CH[BO <sub>2</sub> C <sub>6</sub> H <sub>4</sub> ]; 6.56 s br, 2H, CH=CH[BO <sub>2</sub> C <sub>6</sub> H <sub>4</sub> ]; 7.10–7.22 m, 7.61–7.73 m, 32H, PPh <sub>3</sub> , CH=CH[BO <sub>2</sub> C <sub>6</sub> H <sub>4</sub> ]; 9.69 dt, <sup>3</sup> J <sub>HH</sub> = 11.7, <sup>3</sup> J <sub>HP</sub> = 1.3, 1H, CH=CH[BO <sub>2</sub> C <sub>6</sub> H <sub>4</sub> ]; 5.79 dt, <sup>3</sup> J <sub>HH</sub> = 11.7, <sup>4</sup> J <sub>HP</sub> = 1.8, 1H, CH=CH[BO <sub>2</sub> C <sub>6</sub> H <sub>4</sub> ]; 6.40 ddd, J <sub>HH</sub> = 8.1, 6.7, 2.1, 1H, CH=CH[BO <sub>2</sub> C <sub>6</sub> H <sub>4</sub> ]; 6.65 m, 2H, CH=CH[BO <sub>2</sub> C <sub>6</sub> H <sub>4</sub> ]; 7.10–7.22 m, 7.61–7.73 m, 20H, PPh <sub>3</sub> ; 7.30 m, 1H, CH=CH[BO <sub>2</sub> C <sub>6</sub> H <sub>4</sub> ]; 7.61–7.73 m, 10H, PPh <sub>3</sub> ; 9.71 dt, <sup>3</sup> J <sub>HH</sub> = 11.7, <sup>3</sup> J <sub>HP</sub> = 1.3, 1H, CH=CH[BO <sub>2</sub> C <sub>6</sub> H <sub>4</sub> ]; 1.98 t, <sup>3</sup> J <sub>HH</sub> = 7.7, 2H, BOCH <sub>2</sub> CH <sub>2</sub> O; 3.25 t, <sup>3</sup> J <sub>HH</sub> = 7.7, 2H, BOCH <sub>2</sub> CH <sub>2</sub> O; 5.40 dt, <sup>3</sup> J <sub>HH</sub> = 11.1, <sup>4</sup> J <sub>HP</sub> = 1.7, 1H, CH=CH[BOCH <sub>2</sub> CH <sub>2</sub> O]; 7.32–7.40 m, 7.62–7.76 m, 30H, PPh <sub>3</sub> ; 9.31 d br, <sup>3</sup> J <sub>HH</sub> = 11.0, 1H, CH=CH[BOCH <sub>2</sub> CH <sub>2</sub> O]
$\text{Ru}(\text{CH}=\text{CH}[\text{BOCH}_2\text{CH}_2\text{O}])\text{Cl}(\text{CO})(\text{PPh}_3)_2$ ( <b>3</b> )	0.19 t, <sup>3</sup> J <sub>HH</sub> = 7.0, 3H, B[OCH <sub>2</sub> CH <sub>3</sub> ] (O-metalated); 1.21 t, <sup>3</sup> J <sub>HH</sub> = 7.0, 3H, B[OCH <sub>2</sub> CH <sub>3</sub> ]; 2.85 qt, <sup>3</sup> J <sub>HH</sub> = 7.0, 2H, B[OCH <sub>2</sub> CH <sub>3</sub> ] (O-metalated); 3.90 qt, <sup>3</sup> J <sub>HH</sub> = 7.0, 2H, B[OCH <sub>2</sub> CH <sub>3</sub> ]; 5.49 dt, <sup>3</sup> J <sub>HH</sub> = 11.1, <sup>4</sup> J <sub>HP</sub> = 1.8, 1H, CH=CHB[OEt] <sub>2</sub> ; 7.30–7.40 m, 7.61–7.77 m, 30H, PPh <sub>3</sub> ; 8.89 dt, <sup>3</sup> J <sub>HH</sub> = 11.0, <sup>3</sup> J <sub>HP</sub> = 2.1, 1H, CH=CHB[OEt] <sub>2</sub>
$\text{Ru}(\text{CH}=\text{CHB}[\text{OEt}][\text{OEt}])\text{Cl}(\text{CO})(\text{PPh}_3)_2$ ( <b>4</b> )	

<sup>a</sup> Coupling constants in hertz. <sup>b</sup> Two O<sub>2</sub>C<sub>6</sub>H<sub>4</sub> resonances obscured beneath PPh<sub>3</sub>.

**Table 3. <sup>13</sup>C NMR Data for Ruthenium Complexes**

complex	<sup>13</sup> C, $\delta$ (ppm) <sup>a</sup>
$\text{Ru}(\text{CH}=\text{CH}[\text{BOC}_6\text{H}_4\text{O}])\text{Cl}(\text{CO})(\text{PPh}_3)_2$ ( <b>2</b> ) recorded at 298 K	122.2 s br, CH=CH[BO <sub>2</sub> C <sub>6</sub> H <sub>4</sub> ]; 128.4 t', <sup>2,4</sup> J <sub>CP</sub> = 9.6, PPh <sub>3</sub> <i>ortho</i> ; 130.1 s, PPh <sub>3</sub> <i>para</i> ; 132.4 t', q, <sup>1,3</sup> J <sub>CP</sub> = 44.4, PPh <sub>3</sub> <i>ipso</i> ; 134.3 t', <sup>3,5</sup> J <sub>CP</sub> = 11.4, PPh <sub>3</sub> <i>meta</i> ; 207.3 t, <sup>2</sup> J <sub>CP</sub> = 10.7, CH=CH[BO <sub>2</sub> C <sub>6</sub> H <sub>4</sub> ]; 207.7 t, q, <sup>2</sup> J <sub>CP</sub> = 17.0, CO
recorded at 250 K <sup>b</sup>	111.3 s, BO <sub>2</sub> C <sub>6</sub> H <sub>4</sub> ; 113.0 s br, CH=CH[BO <sub>2</sub> C <sub>6</sub> H <sub>4</sub> ]; 115.7 s, BO <sub>2</sub> C <sub>6</sub> H <sub>4</sub> ; 121.4 s, BO <sub>2</sub> C <sub>6</sub> H <sub>4</sub>
$\text{Ru}(\text{CH}=\text{CH}[\text{BOC}_6\text{H}_4\text{O}])\text{Cl}(\text{CO})(\text{PPh}_3)_2$ ( <b>2</b> ) recorded at 250 K <sup>b</sup>	121.9 s, BO <sub>2</sub> C <sub>6</sub> H <sub>4</sub> ; 128.0 t', <sup>2,4</sup> J <sub>CP</sub> = 10.1, PPh <sub>3</sub> <i>ortho</i> ; 129.5 s, PPh <sub>3</sub> <i>para</i> ; 131.8 t', q, <sup>1,3</sup> J <sub>CP</sub> = 44.3, PPh <sub>3</sub> <i>ipso</i> ; 133.7 t', <sup>3,5</sup> J <sub>CP</sub> = 11.1, PPh <sub>3</sub> <i>meta</i> ; 145.1 s, q, BO <sub>2</sub> C <sub>6</sub> H <sub>4</sub> ; 146.9 s, q, BO <sub>2</sub> C <sub>6</sub> H <sub>4</sub> ; 207.1 t, <sup>2</sup> J <sub>CP</sub> = 10.8, CH=CH[BO <sub>2</sub> C <sub>6</sub> H <sub>4</sub> ]
$\text{Ru}(\text{CH}=\text{CH}[\text{BOCH}_2\text{CH}_2\text{O}])\text{Cl}(\text{CO})(\text{PPh}_3)_2$ ( <b>3</b> )	61.8 s, BOCH <sub>2</sub> CH <sub>2</sub> O; 65.6 s, BOCH <sub>2</sub> CH <sub>2</sub> O; 113.3 s br, CH=CH[BOCH <sub>2</sub> CH <sub>2</sub> O]; 128.1 t', <sup>2,4</sup> J <sub>CP</sub> = 9.1, PPh <sub>3</sub> <i>ortho</i> ; 129.7 s, PPh <sub>3</sub> <i>para</i> ; 133.0 t', q, <sup>1,3</sup> J <sub>CP</sub> = 43.3, PPh <sub>3</sub> <i>ipso</i> ; 134.3 t', <sup>3,5</sup> J <sub>CP</sub> = 11.1, PPh <sub>3</sub> <i>meta</i> ; 203.9 t, <sup>2</sup> J <sub>CP</sub> = 10.6, CH=CH[BOCH <sub>2</sub> CH <sub>2</sub> O]; 207.2 t, q, <sup>2</sup> J <sub>CP</sub> = 17.1, CO
$\text{Ru}(\text{CH}=\text{CHB}[\text{OEt}][\text{OEt}])\text{Cl}(\text{CO})(\text{PPh}_3)_2$ ( <b>4</b> )	14.1 s, B[OCH <sub>2</sub> CH <sub>3</sub> ] (O-metalated); 17.5 s, B[OCH <sub>2</sub> CH <sub>3</sub> ]; 60.5 s, B[OCH <sub>2</sub> CH <sub>3</sub> ] (O-metalated); 61.8 s, B[OCH <sub>2</sub> CH <sub>3</sub> ]; 117.3 s br, CH=CHB[OEt] <sub>2</sub> ; 128.1 t', <sup>2,4</sup> J <sub>CP</sub> = 8.0, PPh <sub>3</sub> <i>ortho</i> ; 129.6 s, PPh <sub>3</sub> <i>para</i> ; 133.3 t', q, <sup>1,3</sup> J <sub>CP</sub> = 42.3, PPh <sub>3</sub> <i>ipso</i> ; 134.5 t', <sup>3,5</sup> J <sub>CP</sub> = 10.1, PPh <sub>3</sub> <i>meta</i> ; 202.7 t, <sup>2</sup> J <sub>CP</sub> = 11.6, CH=CHB[OEt] <sub>2</sub> ; 206.6 t, q, <sup>2</sup> J <sub>CP</sub> = 18.6, CO

<sup>a</sup> Coupling constants in hertz. <sup>b</sup> CO not observed.

= 1.8 Hz. Larger  $J_{\text{HP}}$  values for H<sub>β</sub> than H<sub>α</sub> have been observed before.<sup>13</sup> The <sup>11</sup>B NMR spectrum (referenced to BF<sub>3</sub>·Et<sub>2</sub>O,  $\delta$  = 0 ppm) showed a broad signal centered at 14.2 ppm which is appropriate for the presence of non-metal-substituted tricoordinate boron and this can be compared with the chemical shift of 45.6 ppm observed for the parent compound, Ru(BO<sub>2</sub>C<sub>6</sub>H<sub>4</sub>)Cl(CO)-(PPh<sub>3</sub>)<sub>2</sub>. This chemical shift for **2**, however, is at least 10 ppm upfield of typical alkenylboronate esters.

Surprisingly, the characteristic <sup>1</sup>H NMR resonances normally associated with a catecholate substituent were not observed at 298 K. Instead, at this temperature

only a very broad resonance centered at 6.56 ppm was seen in the <sup>1</sup>H NMR spectrum. However, as the temperature was lowered to 230 K, this broad signal split into two sets of multiplets (see Table 2). Furthermore, an additional multiplet appeared at 7.30 ppm between the resonances of the phenyl protons of the triphenylphosphine ligands. These three resonances account for all four catechol protons as measured by peak integrals.

Likewise, the <sup>13</sup>C NMR spectrum at 298 K showed no signals for the catechol substituent. However, at the lower temperature of 250 K, four methine and two qua-

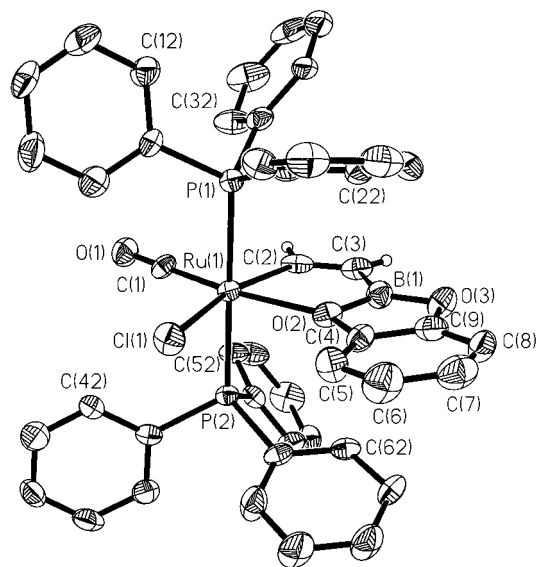


**Figure 1.** Molecular structure of  $\text{Ru}(\text{CH}=\text{CH}[\text{BOC}_6\text{H}_4\text{O}])\text{Cl}(\text{CO})(\text{PPh}_3)_2$  (**2**) showing atoms as 50% probability ellipsoids. Each phenyl ring is numbered from  $C_{n1}$  (attached to P) to  $C_{n6}$  as indicated.

ternary resonances were observed for this fragment. This indicates that at this temperature the six ring carbon atoms are magnetically inequivalent and that the symmetry of the free catecholate group has been lowered.

These variable-temperature  $^1\text{H}$  and  $^{13}\text{C}$  NMR data are consistent with the catecholboryl group coordinating to ruthenium through one oxygen atom but also undergoing a dynamic process in which the oxygen dissociates from ruthenium, the catecholate group rotates about the  $\text{B}-\text{C}_\beta$  bond, and the other oxygen atom then coordinates to ruthenium. This process is rapid at 298 K on both the  $^1\text{H}$  and  $^{13}\text{C}$  NMR time scales, but at 230 K where it is slow, each of the unique ring atoms of the coordinated catecholate group can be observed.

In order to confirm the bidentate coordination mode of the vinyl boronate ester moiety, and to verify unambiguously that insertion of ethyne into the  $\text{Ru}-\text{B}$  bond had occurred, a single-crystal X-ray diffraction study of **2** was undertaken.

#### X-ray Crystal Structure of $\text{Ru}(\text{CH}=\text{CH}[\text{BOC}_6\text{H}_4\text{O}])\text{Cl}(\text{CO})(\text{PPh}_3)_2$ (**2**).

The molecular structure of  $\text{Ru}(\text{CH}=\text{CH}[\text{BOC}_6\text{H}_4\text{O}])\text{Cl}(\text{CO})(\text{PPh}_3)_2$  is depicted in Figure 1. The molecular geometry about ruthenium is approximately octahedral. The ruthenium atom is bonded to two mutually *trans* triphenylphosphine ligands, a carbonyl, a chloride, and a bidentate vinyl catecholboronate ester group. The geometry about the double bond of this latter group is *Z* and coordination to ruthenium is through an alkenyl carbon atom and one of the oxygen atoms of the catechol group. Accordingly, this makes the complex coordinatively saturated. The major distortion from ideal octahedral geometry is associated with the bonding requirements of the vinyl catecholboronate ester ligand with the angle  $\text{C}(2)-\text{Ru}-\text{O}(2)$  being  $77.01(29)^\circ$ .

The  $\text{Ru}-\text{P}$  distances of  $2.390(2)$  and  $2.388(2)$  Å are typical of those observed for other ruthenium(II) com-

plexes that contain mutually *trans* triphenylphosphine ligands.<sup>14</sup> The  $\text{P}(1)-\text{Ru}-\text{P}(2)$  angle is  $179.32(7)^\circ$ , showing essentially linear geometry for the two phosphine ligands. The carbonyl carbon atom is bonded to ruthenium at a distance of  $1.801(8)$  Å, and this is close to the average distance found for other terminal carbonyls coordinated to ruthenium(II). The  $\text{Ru}-\text{Cl}$  distance ( $2.476(2)$  Å) is slightly longer than the mean bond distance found for terminal  $\text{Ru(II)-Cl}$  bonds and this probably reflects the *trans* labilising influence of the alkenyl group.<sup>14</sup> The alkenyl carbon,  $\text{C}(2)$ , is bonded to the ruthenium at a distance of  $2.055(8)$  Å, which is very similar to the corresponding distances observed in the  $\sigma$ -bonded alkenyl complexes,  $\text{Ru}(\eta^2\text{-O}_2\text{CMe})(\text{HCCPh})(\text{CO})(\text{PPh}_3)_2$  ( $2.030(15)$  Å) and  $\text{RuCl}(\text{PhC}=\text{CHPh})(\text{CO})(\text{PPh}_3)_2$  ( $2.03(1)$  Å).<sup>12,15</sup> The *Z* geometry at the double bond allows a close approach of the boronate ester to the metal affording a dative bonding interaction between a catecholate oxygen atom and ruthenium. The  $\text{Ru}-\text{O}$  bond length is  $2.275(6)$  Å, and this is shorter than those found in the  $\eta^2$ -acyl complexes  $\text{RuI}(\eta^2\text{-C[O]Me})(\text{CO})(\text{PPh}_3)_2$  ( $2.47(2)$  Å) or  $\text{RuI}(\eta^2\text{-C[O]-p-tolyl})(\text{CO})(\text{PPh}_3)_2$  ( $2.36(1)$  Å)<sup>16</sup> but similar to that found in  $\text{RuCl}(\text{MeO[O]CC}=\text{C}\{\text{C[O]OMe}\}\text{CH}=\text{CHCMe}_3)(\text{CO})(\text{PPh}_3)_2$  ( $2.291(9)$  Å), which was derived from the insertion of dimethylacetylenedicarboxylate into the alkenyl complex  $\text{RuCl}(\text{CH}=\text{CHCMe}_3)(\text{CO})(\text{PPh}_3)_2$ .<sup>17</sup> In comparison to typical ruthenium-oxygen single bond distances,<sup>14</sup> however, this bond length is very long, indicating only a modest bonding interaction between oxygen and ruthenium.

The catecholboryl fragment and the ethenyl unit to which it is bonded are coplanar. The  $\text{C}(2)-\text{C}(3)$  bond length of  $1.266(12)$  Å is appropriate for a double bond. Both hydrogen atoms were located in the Fourier difference map and are shown in Figure 1. Other bonds within the catecholboryl unit are normal.

A recent *ab initio* theoretical study of the  $\text{RhCl}(\text{PPh}_3)_2$ -catalyzed hydroboration of alkenes<sup>8g</sup> revealed that the most favorable pathway involves oxidative addition of the borane to the Rh center followed by insertion of ethene into the  $\text{Rh}-\text{B}$  bond. The calculated structure of the resulting intermediate complex,

$\text{Rh}(\text{CH}_2\text{CH}_2\text{B}[\text{OH}][\text{OH}])\text{HCl}(\text{PPh}_3)_2$ , is very similar to that found for  $\text{Ru}(\text{CH}=\text{CH}[\text{BOC}_6\text{H}_4\text{O}])\text{Cl}(\text{CO})(\text{PPh}_3)_2$ . In the calculated structure, one of the oxygen atoms bonded to boron interacts weakly with the rhodium center and the  $\text{Rh}-\text{O}$  bond distance is  $2.26$  Å (cf.  $2.275(6)$  Å for **2**). Complex **2** therefore serves as a useful model for one of the key intermediates in some metal-catalyzed alkene and alkyne hydroboration reactions. Furthermore, the observation that ethyne formally inserts into the  $\text{Ru}-\text{B}$  bond of **1** to give the borylalkenyl complex **2** indicates that it is entirely feasible that this process could also occur as a key step in metal-catalyzed hydroboration reactions of alkynes and, by inference, alkenes.

We have no information regarding details of the mechanism by which ethyne inserts into the  $\text{Ru}-\text{B}$  bond

(14) From a search of the Cambridge Crystallographic Database.

(15) Loumhari, H.; Perales, A.; Ros, J.; Torres, M. R. *J. Organomet. Chem.* **1990**, 385, 379.

(16) Roper, W. R.; Taylor, G. E.; Waters, J. M.; Wright, L. J. *J. Organomet. Chem.* **1979**, 182, C46.

(17) Ros, J.; Santos, A.; Torres, M. R.; Vegas, A. *J. Organomet. Chem.* **1987**, 326, 413.

of **1** to give **2**. However, if ethyne initially adds *trans* to the boryl ligand in **1**, then it would be necessary that an isomerization brings the boryl and ethyne ligands mutually *cis* before formal insertion could occur.

**Substitution at the Boron Center of Ru(CH=CH[BOC<sub>6</sub>H<sub>4</sub>O])Cl(CO)(PPh<sub>3</sub>)<sub>2</sub>.** In compound **1** where the catecholboryl group is directly bonded to ruthenium, the boron center shows no reactivity toward alcohols. In contrast, the compound **2** readily undergoes substitution chemistry centered at boron. This reaction chemistry is typically associated with organoboronate esters, where transesterification with other alcohols may be accomplished with relative ease. However, on treatment of **2** with simple alcohols like methanol or ethanol, only complex mixtures of products were produced which could not be easily separated. Therefore, reaction with the diol 1,2-dihydroxyethane (ethylene glycol) was investigated. This reagent is often used in organic synthesis for the preparation of boronic esters via esterification of boronic acids, and it is known to form very stable cyclic derivatives.<sup>18</sup>

Treatment of Ru(CH=CH[BOC<sub>6</sub>H<sub>4</sub>O])Cl(CO)(PPh<sub>3</sub>)<sub>2</sub> with ethylene glycol in a dichloromethane/ethanol solution resulted in formation of a colorless product, Ru(CH=CH[BOCH<sub>2</sub>CH<sub>2</sub>O])Cl(CO)(PPh<sub>3</sub>)<sub>2</sub> (**3**) (see Scheme 1). The infrared spectrum of this product displayed a sharp  $\nu(\text{CO})$  band at 1907 cm<sup>-1</sup> as well as other significant bands at 1492, 1403, 1247, 1190, and 1014 cm<sup>-1</sup>. The <sup>1</sup>H NMR spectrum confirmed that transesterification had taken place. The broad resonance associated with the catechol moiety at 6.56 ppm was replaced by two new triplet resonances at 1.98 and 3.25 ppm each of which integrated for two protons. These resonances were assigned to the two sets of methylene protons of the dioxaborolidine moiety. The appearance of two signals and the nearly colorless nature of the complex is again consistent with a bonding interaction between ruthenium and an oxygen of the dioxaborolidine ligand. The ethenyl proton resonances were observed at 5.40 and 9.31 ppm. Both signals were observed as doublets (<sup>3</sup>J<sub>HH</sub> = 11 Hz) of triplets, although the smaller coupling to phosphorus for the lower field signal was not well resolved. The assignments of these resonances were made by comparison with the assignments made for the corresponding signals in **2** (see Table 2).

The <sup>13</sup>C NMR spectra corroborated the above formulation for **3** and the presence of the two methylene carbon resonances was observed at 61.8 and 65.6 ppm. The assignment of the methylene signals was confirmed by a DEPT 135 experiment. A broad singlet at 113.3 ppm was assigned to the ethenyl carbon attached to boron, and a triplet resonance centered at 203.9 ppm was assigned to the ethenyl carbon bound directly to the metal with <sup>2</sup>J<sub>CP</sub> = 10.6 Hz.

The observation of sharp, well-resolved signals for the two methylene groups in both the <sup>1</sup>H and <sup>13</sup>C NMR spectra at 298 K shows that any rotation about the C–B bond in **3** is very slow on the corresponding NMR time scales. This is in contrast to the situation for **2** (see

above) and may be because the oxygen atoms of the aliphatic diol group are much better donors toward ruthenium than the oxygens of the catechol group. The enhanced basicity of the oxygen atoms in **3** may also be responsible for the increased stability of the dioxaborolidine group toward transesterification. It was found that **3** could be recrystallized from dichloromethane/ethanol without exchange of the diol occurring.

Attempts to carbonylate Ru(CH=CH[BOC<sub>6</sub>H<sub>4</sub>O])Cl(CO)(PPh<sub>3</sub>)<sub>2</sub> led only to mixtures of products that could not be separated or identified. On the other hand, treatment of a dichloromethane solution of Ru(CH=CH[BOCH<sub>2</sub>CH<sub>2</sub>O])Cl(CO)(PPh<sub>3</sub>)<sub>2</sub> with CO followed by addition of ethanol afforded a colorless, microcrystalline product in moderate yield. Rather than the anticipated dicarbonyl derivative, "Ru(CH=CH[BOCH<sub>2</sub>CH<sub>2</sub>O])Cl(CO)<sub>2</sub>(PPh<sub>3</sub>)<sub>2</sub>," this complex was determined to be Ru(CH=CHB[OEt][OEt])Cl(CO)(PPh<sub>3</sub>)<sub>2</sub> (**4**), the bis-(ethoxy) boronate ester analogue of the parent diol complex **3** (see Scheme 1).

The one carbonyl ligand in **4** gives rise to one sharp  $\nu(\text{CO})$  band in the IR spectrum at 1914 cm<sup>-1</sup> and other significant bands occur at 1320, 1266, 1207, 1028, 885, and 724 cm<sup>-1</sup>. Doublet of triplet resonances in the <sup>1</sup>H NMR spectrum at both 5.49 and 8.89 ppm were assigned to the two protons of the ethenyl group, and a broad singlet at 117.3 ppm and a sharp triplet at 202.7 ppm in the <sup>13</sup>C NMR spectrum were assigned to the two carbon atoms of this same group. In place of the two triplet resonances observed in the <sup>1</sup>H NMR spectrum for the two methylene groups in **3**, two triplet (0.19 and 1.21 ppm) and two quartet (2.85 and 3.90 ppm) resonances were found for **4**. These were assigned to the two ethoxy groups attached to boron. The inequivalence of these two groups arises because the oxygen atom of one of the ethoxy groups is coordinated to ruthenium. As for **3**, rotation about the C–B bond in **4** must also be slow on the NMR timescale.

Compound **4** can also be formed by treatment of a dichloromethane solution of **3** with acetonitrile and ethanol, although this procedure gives a lower yield of **4**. In the absence of CO or acetonitrile, **3** can be recovered unchanged from dichloromethane/ethanol solutions. It is possible that the role of the CO or acetonitrile in promoting alkoxide group exchange at boron is to displace the coordinated oxygen from the metal center and thereby facilitate attack at the boron center. Alternatively, these Lewis bases may displace the chloride from the metal, and the resulting cationic species may then display a much higher susceptibility to nucleophilic attack by ethanol. In either case, the initial Lewis base coordination would then have to be reversed after the ethanolysis and this could possibly occur during the product isolation step.

**Reaction of Compound 2 with HBO<sub>2</sub>C<sub>6</sub>H<sub>4</sub>.** Since opening the chelate ring in **2** produces a five-coordinate organoruthenium compound of the type RuRCl(CO)(PPh<sub>3</sub>)<sub>2</sub> (in this case R = CH=CHBO<sub>2</sub>C<sub>6</sub>H<sub>4</sub>), it was to be expected that reaction with HBO<sub>2</sub>C<sub>6</sub>H<sub>4</sub> would result in formation of the "parent" boryl complex **1**.<sup>11</sup> This expectation was confirmed, and when **2** was treated with HBO<sub>2</sub>C<sub>6</sub>H<sub>4</sub> in benzene under reflux for 30 min, **1**

(18) Bhat, N. G.; Brown, H. C.; Somayaji, V. *Organometallics* **1983**, 2, 1311.

was produced in nearly quantitative yield. This observation could be relevant for the development of compounds like **1** as hydroboration catalysts.

**Investigations of Other Closely Related Insertion Reactions.** The generality of the ethyne insertion reaction involved in the formation of **2** was tested by examining reactions with other related metal–boryl complexes. No pure products could be isolated from treatment of either  $\text{Ru}(\text{B}[\text{NH}]_2\text{C}_6\text{H}_4)\text{Cl}(\text{CO})(\text{PPh}_3)_2^{11}$  or  $\text{Ru}(\text{B}[\text{NH}]\text{SC}_6\text{H}_4)\text{Cl}(\text{CO})(\text{PPh}_3)_2^{11}$  with ethyne. In contrast, the osmium–boryl complex  $\text{Os}(\text{BO}_2\text{C}_6\text{H}_4)\text{Cl}(\text{CO})(\text{PPh}_3)_2^{11}$  did give an isolable product with this alkyne but with loss of the boryl group. The product proved to have an  $\eta^3$ -allylic moiety which was derived from the cyclotrimerization of acetylene. This product will be the subject of a separate paper.

The possibility of inserting other unsaturated substrates into the Ru–B bond of **1** was also investigated. The terminal alkynes, 1-propyne and 1-butyne, both gave insertion products, and the full characterization of these compounds is currently being studied. In contrast, no tractable boryl-containing products were isolated when **1** was treated with phenylacetylene, diphenylacetylene, 2-butyne, dimethylacetylenedicarboxylate, propargyl alcohol, ethene, cyclohexene, carbon dioxide, and sulfur dioxide.

### Summary and Conclusions

The complex  $\text{Ru}(\text{CH}=\text{CH}[\text{BOC}_6\text{H}_4\text{O}])\text{Cl}(\text{CO})(\text{PPh}_3)_2$  (**2**) is the first example of a structurally characterized product resulting from the stoichiometric, formal insertion of an unsaturated molecule into a metal–boron bond. This complex has been fully characterized by IR and multinuclear NMR spectroscopies as well as by single-crystal X-ray diffraction analysis. The geometry about the double bond of the vinylboronate ligand is *Z* with an oxygen of the catecholboryl group interacting weakly with the metal. Variable-temperature NMR spectroscopy shows that the catecholboryl group undergoes a dynamic process in solution which can be explained in terms of rotation about the  $\text{C}_\beta$ –B bond. The observation that ethyne formally inserts into the Ru–B bond of **1** to give the alkenyl complex **2** indicates it is feasible that such a process could also occur in some metal-catalyzed hydroboration reactions of alkynes and, by inference, alkenes.

The complex  $\text{Ru}(\text{CH}=\text{CH}[\text{BOCH}_2\text{CH}_2\text{O}])\text{Cl}(\text{CO})(\text{PPh}_3)_2$  (**3**) was prepared via a facile transesterification reaction of  $\text{Ru}(\text{CH}=\text{CH}[\text{BOC}_6\text{H}_4\text{O}])\text{Cl}(\text{CO})(\text{PPh}_3)_2$  (**2**) with ethylene glycol. In contrast, no catecholate substitution reactions were observed under similar conditions for **1** where the boron atom is directly bonded to ruthenium. Although the boron center is more sterically protected in **1** than in **2**, the major factor responsible for this reduced reactivity is most probably the reduced electrophilicity of the boron that results from the direct interaction with ruthenium.

The increased basicity of the ethanediol group oxygen atoms in **3**, compared to the catecholate oxygens in **2**, reduces the susceptibility of the boron center toward nucleophilic attack in **3**. Therefore, unlike **2**, **3** can be recrystallized unchanged in the presence of ethanol.

**Table 4. Crystal Data and Structure Refinement for  $\text{Ru}(\text{CH}=\text{CH}[\text{BOC}_6\text{H}_4\text{O}])\text{Cl}(\text{CO})(\text{PPh}_3)_2 \cdot 2.5\text{C}_6\text{H}_6$  (**2**)**

empirical formula	$\text{C}_{45}\text{H}_{36}\text{BClO}_3\text{P}_2\text{Ru} \cdot 2.5\text{C}_6\text{H}_6$
formula weight	1029.28
temperature	193(2) K
wavelength	0.710 69 Å
cryst syst	$P2_1/c$
space group	monoclinic
unit cell dimens	$a = 13.381(5)$ Å, $b = 13.601(2)$ Å, $c = 27.907(6)$ Å; $\alpha = 90.00^\circ$ , $\beta = 102.36(2)^\circ$ , $\gamma = 90.00^\circ$
volume	$4961(2)$ Å <sup>3</sup>
<i>Z</i>	4
density (calcd)	$1.378$ mg m <sup>−3</sup>
absorption coeff	$0.491$ mm <sup>−1</sup>
range of absorptn corrns	$0.777$ – $1.000$
<i>F</i> (000)	2116
crystal size	$0.31 \times 0.19 \times 0.09$ mm, off-white needles
$\theta$ range for data collection	$1.49$ – $25.97^\circ$
index ranges	$-16 \leq h \leq 0$ , $-16 \leq k \leq 0$ , $-33 \leq l \leq 34$
no. of reflctns collected	10 116
no. of independent reflctns	9665 [ $R(\text{int}) = 0.0372$ ]
refinement method	full-matrix least-squares on $F^2$
data/restraints/parameters	9650/0/712
goodness of fit on $F^2$	1.023
final <i>R</i> indices [ $I > 2\sigma(I)$ ]	$R1 = 0.0672$ , $wR2 = 0.1715$
<i>R</i> indices (all data)	$R1 = 0.1611$ , $wR2 = 0.2295$
largest diff peak and hole	$1.893$ and $-0.954$ e Å <sup>−3</sup>

However, ethanol displaces the ethanediol group in **3** in the presence of CO or acetonitrile and the bis(ethoxy)-

boronate ester complex  $\text{Ru}(\text{CH}=\text{CHB}[\text{OEt}][\text{OEt}])\text{Cl}(\text{CO})(\text{PPh}_3)_2$  (**4**) is formed. Displacement of the coordinated oxygen atom from ruthenium in **3** by CO or acetonitrile or the formation of a cationic complex through chloride displacement may be responsible for the increased reactivity of the boron center in this case.

### Experimental Section

**General Considerations.** The general experimental and spectroscopic techniques employed in this work were the same as those described previously.<sup>11,13</sup>

**$\text{Ru}(\text{CH}=\text{CH}[\text{BOC}_6\text{H}_4\text{O}])\text{Cl}(\text{CO})(\text{PPh}_3)_2$  (**2**).**  $\text{Ru}(\text{BO}_2\text{C}_6\text{H}_4)\text{Cl}(\text{CO})(\text{PPh}_3)_2^{11}$  (1.200 g, 1.485 mmol) was added to benzene (40 mL) in a Fisher-Porter bottle and placed under a pressure of  $\text{C}_2\text{H}_2$  (1 atm) (CAUTION, potential explosion hazard). The solution was then heated to  $\sim 65^\circ\text{C}$  for 20 min or until such time as any suspended starting material had dissolved. The resulting clear golden yellow solution was reduced in volume *in vacuo* to  $\sim 8$  mL. Slow addition of *n*-hexane effected the crystallization of an off-white microcrystalline solid. Following filtration, the solid was then washed with several small portions of *n*-hexane. The product at this point was sufficiently pure for conversion to the other derivatives described below; however, for microanalysis it was recrystallized from benzene/*n*-hexane (1.194 g, 96 %). Anal. Calcd for  $\text{C}_{45}\text{H}_{36}\text{BClO}_3\text{P}_2\text{Ru}$ : C, 64.80; H, 4.35; Cl, 4.25. Found C, 64.84; H, 4.24; Cl, 3.96. A crystal suitable for X-ray study (see below) was grown from benzene and proved to be the benzene solvate,  $\text{Ru}(\text{CH}=\text{CH}[\text{BOC}_6\text{H}_4\text{O}])\text{Cl}(\text{CO})(\text{PPh}_3)_2 \cdot 2.5\text{C}_6\text{H}_6$ .

**$\text{Ru}(\text{CH}=\text{CH}[\text{BOCH}_2\text{CH}_2\text{O}])\text{Cl}(\text{CO})(\text{PPh}_3)_2$  (**3**).**  $\text{Ru}(\text{CH}=\text{CH}[\text{BOC}_6\text{H}_4\text{O}])\text{Cl}(\text{CO})(\text{PPh}_3)_2$  (0.325 g, 0.390 mmol) was added to a mixture of ethanol (20 mL) and ethylene glycol (1 mL). The resulting suspension was then stirred rapidly while

**Table 5. Selected Interatomic Distances (Å) for Ru(CH=CH[BOC<sub>6</sub>H<sub>4</sub>O])Cl(CO)(PPh<sub>3</sub>)<sub>2</sub> (2)**

bond	distance	bond	distance
Ru–P(1)	2.390(2)	C(1)–O(1)	1.147(9)
Ru–P(2)	2.388(2)	O(2)–C(4)	1.406(9)
Ru–Cl	2.476(2)	O(3)–C(9)	1.376(10)
Ru–O(2)	2.275(6)	C(4)–C(5)	1.373(12)
Ru–C(1)	1.801(8)	C(5)–C(6)	1.379(13)
Ru–C(2)	2.055(8)	C(6)–C(7)	1.380(15)
C(2)–C(3)	1.266(12)	C(7)–C(8)	1.376(14)
C(3)–B	1.535(12)	C(8)–C(9)	1.394(12)
B–O(2)	1.413(11)	C(4)–C(9)	1.393(12)
B–O(3)	1.384(11)		

dichloromethane was added to effect dissolution (~35 mL). The resulting yellow-brown mixture was stirred at room temperature for 5–10 min. Slow evaporation of solvent under reduced pressure gave a gray microcrystalline precipitate. Recrystallization from dichloromethane/ethanol afforded nearly

colorless microcrystals of Ru(CH=CH[BOCH<sub>2</sub>CH<sub>2</sub>O])Cl(CO)-(PPh<sub>3</sub>)<sub>2</sub> (0.145 g, 47 %). The <sup>1</sup>H NMR spectrum of this sample indicated 0.5 equiv of water solvate. Anal. Calcd for C<sub>41</sub>H<sub>36</sub>BClO<sub>3</sub>P<sub>2</sub>Ru·H<sub>2</sub>O: C, 61.94; H, 4.69. Found C, 62.11; H, 4.91.

**Ru(CH=CHB[OEt][OEt])Cl(CO)(PPh<sub>3</sub>)<sub>2</sub> (4).** Ru(CH=CH-[BOCH<sub>2</sub>CH<sub>2</sub>O])Cl(CO)(PPh<sub>3</sub>)<sub>2</sub> (0.050 g, 0.064 mmol) was dissolved in dichloromethane (10 mL) and the solution added to a Fisher-Porter bottle. This was then rapidly pressurized with carbon monoxide (4 atm) at room temperature while being stirring vigorously. After 5 min the pressure was released and ethanol was added. Slow reduction of the solvent volume on a rotary evaporator resulted in crystallization of the nearly colorless product. Recrystallization from dichloromethane/ethanol gave colorless crystals of Ru(CH=CHB[OEt][OEt])Cl(CO)(PPh<sub>3</sub>)<sub>2</sub> (0.022 g, 42 %). The <sup>1</sup>H NMR spectrum of this sample indicated 1.5 equiv of water solvate. Anal. Calcd for C<sub>43</sub>H<sub>42</sub>BClO<sub>3</sub>P<sub>2</sub>Ru·F(3,2) H<sub>2</sub>O: C, 61.26; H, 5.38. Found C, 61.09; H, 5.19.

**X-ray Diffraction Study of Compound 2.** A crystal suitable for intensity data collection was mounted on a glass fiber and positioned on a Nonius CAD-4 diffractometer. Unit cell dimensions were derived from least-squares fits to the observed setting angles of 25 reflections distributed throughout reciprocal space, using monochromated Mo K $\alpha$  radiation at 193(2) K. Intensity data collection employed the 2 $\theta$ / $\omega$  technique with a total peak/background count time of 2:1. Reflections were counted for 60 s or until  $\sigma(I)/I$  was 0.02. Crystal alignment and decomposition were monitored throughout data collection by measuring three standard reflections every 100 measurements; no statistically significant variation was observed. The data were corrected for Lorentz and polarization effects. Absorption corrections were applied using  $\psi$  scans<sup>19</sup> and equivalent reflections averaged. Details of crystal data and intensity data collection parameters are summarized in

**Table 6. Selected Bond Angles (deg) for Ru(CH=CH[BOC<sub>6</sub>H<sub>4</sub>O])Cl(CO)(PPh<sub>3</sub>)<sub>2</sub> (2)**

bond	angle	bond	angle
P(1)–Ru–P(2)	179.32(7)	C(1)–Ru–O(2)	170.88(27)
P(1)–Ru–Cl	92.75(7)	C(2)–Ru–O(2)	77.01(29)
P(1)–Ru–C(1)	89.02(25)	Ru–C(1)–O(1)	177.71(65)
P(1)–Ru–C(2)	89.09(21)	Ru–C(2)–C(3)	122.07(65)
P(1)–Ru–O(2)	89.49(14)	Ru–O(2)–B	109.37(49)
P(2)–Ru–Cl	87.92(7)	Ru–O(2)–C(4)	144.94(49)
P(2)–Ru–C(1)	90.73(25)	C(2)–C(3)–B	115.95(78)
P(2)–Ru–C(2)	90.30(21)	C(3)–B–O(2)	115.49(77)
P(2)–Ru–O(2)	91.66(14)	C(3)–B–O(3)	133.51(81)
Cl–Ru–C(1)	102.30(24)	O(2)–B–O(3)	110.96(73)
Cl–Ru–C(2)	163.64(26)	B–O(2)–C(4)	105.39(64)
Cl–Ru–O(2)	86.75(15)	B–O(3)–C(9)	105.36(68)
C(1)–Ru–C(2)	93.98(35)		

Table 4. Selected interatomic distances (Å) are listed in Table 5, and selected bond angles (deg) are listed in Table 6.

The structure was solved by Patterson and electron density syntheses. Refinement on  $F^2$  employed SHELXL-93,<sup>20</sup> minimizing the function  $\sum w|F_o|^2 - |F_c|^2|^2$ . Atomic scattering factors were for neutral atoms.<sup>21</sup> After initial isotropic refinement, anisotropic thermal parameters were refined for all non-hydrogen atoms. The X-ray analysis showed the presence of 2.5 benzene molecules of solvation, and these were included in all subsequent calculations. Thirteen hydrogen atoms were placed in calculated positions and refined using the riding model; a further 29 hydrogens (including the two ethenyl hydrogens) were located in a difference map and refined as individual atoms with isotropic temperature factors. The two hydrogen atoms on the ethenyl group refined to C–H distances of 0.837 and 0.838 Å. There was disorder apparent in the benzene rings and atoms C(82) and C(83) were each split into two half-atoms to better model that ring.

Weights used in the least-squares refinement were  $w = 1/[(\sigma^2(F_o)^2 + (aP)^2 + bP)]$ , where  $P = [(F_o)^2 + 2(F_c)^2]/3$ , and the final values of  $a$  and  $b$  are 0.122 and 8.08 respectively.

**Acknowledgment.** We thank The University of Auckland Research Committee for partial support of this work through grants-in-aid.

**Supporting Information Available:** Tables of atomic coordinates, bond lengths and angles, anisotropic thermal parameters, and hydrogen atom positions for **2** (9 pages). See any current masthead page for ordering and Internet access instructions.

OM970618Q

(19) North, A. C. T.; Phillips, D. C.; Mathews, F. S. *Acta Crystallogr.* **1968**, A24, 351.

(20) Sheldrick, G. M. *SHELXL93. Program for the Refinement of Crystal Structures*. Univ. of Göttingen, Germany, 1993.

(21) Atomic Scattering Factors are from *International Tables for X-ray Crystallography*, Kynoch Press: Birmingham, England 1992; Vol. C.